

Protein Dynamics in Photosystem II Complexes of Green Plants Studied by Time-Resolved Hole-Burning

F. T. H. den Hartog,[†] C. van Papendrecht,^{†,‡} U. Störkel,^{†,§} and S. Völker^{*,†,||}

Center for the Study of Excited States of Molecules, Huygens and Gorlaeus Laboratories, University of Leiden, P.O. Box 9504, 2300 RA Leiden, The Netherlands, and Department of Biophysics, Faculty of Exact Sciences, Free University, De Boelelaan 1081, 1081 HV Amsterdam, The Netherlands

Received: November 19, 1998

We have studied the protein dynamics of three subcore reaction-center complexes of photosystem II: the isolated reaction center (RC), the core antenna CP47, and the CP47 RC complex by means of time-resolved hole-burning in the red wing of their Q_y -absorption bands. The dependence of the “effective” homogeneous line width Γ'_{hom} on temperature T between 1.2 and 4.2 K suggests that optical dephasing in these proteins is determined by two-level systems (TLSs), as in doped organic glasses. By contrast, the increase of Γ'_{hom} as a function of delay time t_d (between burning and probing the hole) from 10^{-5} to 10^5 s, caused by spectral diffusion (SD), differs from that in glasses and is characteristic for each complex. CP47 RC does not undergo any SD over 10 decades in time for $T \leq 4.2$ K, i.e., $\Gamma'_{\text{hom}} = \text{constant}$ at a given temperature. Although CP47 and the RC do not show SD for $t_d \leq 1$ s, they do for longer delay times, with Γ'_{hom} increasing logarithmically with t_d . The onset and amount of SD appear to be correlated with the mass of the protein. We conclude that only slow motions, related to TLSs located at the more flexible surface of the protein (with a broad and continuous distribution of rates $R < 1\text{--}3$ Hz), contribute to SD at long delay times and that the whole protein, or a substantial part of it, is involved in SD. Fast, local fluctuations associated with a rigid, crystalline-like inner protein core are responsible for “pure” dephasing at short t_d .

1. Introduction

One of the aims of studying conformational dynamics of proteins is to get further insight into their structure–function relation. Proteins in their native state have a well-defined tertiary structure and are ordered like crystalline systems. But to perform a biological function they have to be flexible and adapt their structure to that function, i.e., they have to undergo conformational changes. Proteins, indeed, assume a large number of slightly different structures, called conformational substates (CSs), separated by energy barriers that can be crossed either by tunneling or thermal activation. Thus, they exhibit structural dynamics by going from one CS to another.^{1,2} Because the distribution of energy barriers is broad, the dynamics of proteins cover a wide range of time scales. The corresponding multidimensional energy surface, called the energy landscape (EL), has a rugged structure superimposed on a deep well.³ ELs are reminiscent of two-level systems (TLSs) in glasses,^{4,5} but the difference is that proteins have structures in which the CSs are supposed to be hierarchically organized;⁶ glasses, by contrast, are randomly disordered.

Because individual protein molecules occupy different CSs and the electronic transition frequency of a pigment bound to the protein depends on its conformation, the optical absorption spectrum of an ensemble of molecules of a given protein is inhomogeneously broadened. The “flipping” from one CS to

another within the inhomogeneous band can be studied by following the shift of the optical resonance frequency as a function of the experimental time scale. This process, which is called spectral diffusion (SD), causes an increase of the “effective” homogeneous line width Γ'_{hom} with time. SD yields information on the conformational dynamics of proteins through the distribution of fluctuation rates $P(R)$. Laser line-narrowing techniques, like photon echoes and spectral hole-burning, are ideal tools to investigate spectral diffusion in pigment–protein complexes.

Thus far, only a few studies have been reported on protein dynamics at low temperature by means of optical spectroscopic methods: three-pulse photon echoes,^{7–10} infrared vibrational echoes from 60 to 300 K,¹¹ temperature-cycling hole-burning in the 100 mK range^{10,12,13} and between 4 and 70 K,¹⁴ and low-resolution transient hole-burning from 180 to 300 K.¹⁵ The proteins investigated were Zn mesoporphyrin IX substituted myoglobin^{8–10} and cytochrome *c*,⁷ wild-type myoglobin,¹¹ and free-base^{10,12–14} and Zn¹⁵ protoporphyrin IX substituted myoglobin. The photon-echo results of refs 7–10 obtained in a time span between 10^{-10} and 10^{-1} s suggested that only a limited number of sharp fluctuation rates are active at low temperatures, in contrast to a continuous distribution of rates found for glasses.^{16–18} Although the nature of the molecular mechanism was not revealed by these photon-echo experiments, it was believed that the discrete relaxation rates observed for myoglobin correspond to conformational fluctuations that involve motions of many atoms and possibly of the whole protein.⁸

Here we present results on the protein dynamics of three subcore complexes of photosystem II (PS II) of green plants between 1.2 and 4.2 K obtained by high-resolution time-resolved spectral hole-burning (HB) covering 10 orders of magnitude in

* To whom correspondence should be addressed.

[†] University of Leiden.

[‡] Present address: Netherlands Measuring Institute, P.O. Box 654, 2600 AR Delft, The Netherlands.

[§] Present address: Hahn-Meitner-Institut Berlin, Glienicke Strasse 100, D-14109 Berlin, Germany.

^{||} Free University.

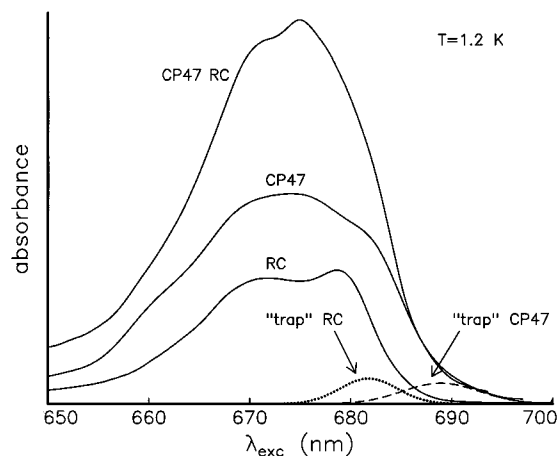


Figure 1. Trap distributions in the absorption spectra of the RC, CP47, and CP47 RC complexes at 1.2 K. The CP47 RC complex has two traps corresponding to the RC and the CP47 components.²⁰

time, from 10^{-5} to 10^5 s. The systems studied are the isolated reaction center (RC), the CP47-core antenna, and the CP47 RC complex.¹⁹ The HB experiments were performed on their "trap" pigments, i.e., pigments not involved in energy transfer and, therefore, characterized by narrow holes. Their widths at temperature $T \rightarrow 0$ are determined by the fluorescence decay time of a few nanoseconds. The spectral distributions of these trap pigments, shown in Figure 1 together with the absorption spectra of the three complexes, have been previously determined.²⁰

The PS II consists of a light-harvesting complex called LHC II²¹ and a central core.¹⁹ The latter includes the reaction center RC,²² where primary charge separation occurs, and several core antenna complexes.²³ The isolated RC is the smallest subunit of PS II that shows photochemical activity. It consists of the D1 and D2 proteins, the cytochrome *b559* polypeptide, and the *psbI* gene product. The proteins bind six chlorophylls *a* (Chl *a*), two pheophytins *a* (Pheo *a*), and one or two β -carotenes.²⁴ The RC has a molecular mass of ~ 110 kDa. The core antenna CP47 is a monomeric protein attached to the RC with a molecular mass of ~ 70 kDa. It comprises probably six hydrophobic transmembrane-spanning α helices²⁵ that bind 13–15 Chl *a* molecules^{26,27} and two β -carotenes. The largest complex, CP47 RC,²⁸ contains 21–23 pigments and has a mass of ~ 180 kDa.

The paper is organized as follows. In the next section, the sample preparation, the time-resolved hole-burning (HB) technique, and the procedure to determine Γ'_{hom} are described. Persistent and transient holes (which decay with the triplet lifetime of about 1 ms) were observed. In the time region where both types of holes can be detected, their widths are equal and, therefore, independent of the HB mechanism.^{16,30} Results are then presented on optical dephasing and spectral diffusion of the trap pigments in the three complexes. It will be shown that although Γ'_{hom} follows a temperature dependence characteristic for organic glassy systems, its functional dependence on delay time differs from that in glasses and is specific for each protein. For short delay times, the behavior is crystalline-like;^{31–34} for long delay times there are slow, glasslike motions.

2. Experimental Section

2.1. Sample Preparation. We have used the same samples as those in ref 20: the PS II subcore complexes CP47 RC, and CP47 and the RC, prepared as described in refs 24, 35, 36. Prior to the low-temperature measurements, the complexes were

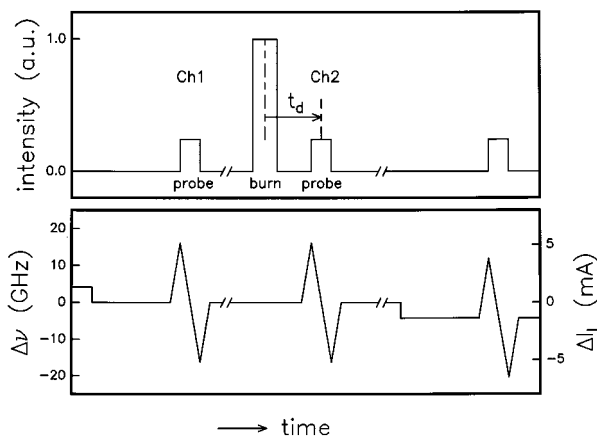


Figure 2. Pulse sequence used in high-resolution time-resolved HB experiments. The delay time t_d between burning and probing a hole is defined in the plot (top figure). The pulse sequence consists of three steps, as described in the text.

diluted in a buffer to an optical density $OD \approx 0.1$ and stored at 77 K when not used.²⁰ The samples were cooled from room temperature to 77 K in about 10 min by keeping the cuvette (thickness 3 mm) in an empty ^4He -bath cryostat of which the outer mantle was filled with liquid nitrogen. Glasses of good optical quality were obtained in this way. Cooling from 77 to 4.2 K was achieved in a few minutes by filling the cryostat with liquid helium. The temperature of the sample, varied between 4.2 and 1.2 K, was controlled by the vapor pressure of ^4He and measured with a calibrated carbon resistor in contact with the sample. The accuracy in the temperature determination was better than 0.01 K.

2.2. High-Resolution Time-Resolved Hole-Burning (HB).

The pulse sequence used in these experiments consists of three steps (see Figure 2):^{16,30} (i) To obtain a baseline before burning, a probe pulse at low intensity is applied during which the frequency of the laser is scanned over the spectral region of interest (see lower part of Figure 2). (ii) To create a hole, a burn pulse at higher intensity (about 100 to 1000 times) is applied during which the frequency of the laser is fixed. (iii) To monitor the hole after a given delay time t_d , a second probe pulse at low intensity is applied during which the frequency of the laser is scanned again over the same spectral region as before burning. The profile of the hole is obtained by subtracting the signals of the first and third pulses. The holewidth is followed for delay times varying between 10^{-5} and 10^5 s.

Two types of lasers were used, depending on the time scale. For delay times shorter than 200 ms, we used one of two current- and temperature-controlled single-mode diode lasers (Toshiba TOLD 9140, $P_{\text{max}} = 20$ mW), depending on excitation wavelength at room temperature of 690 nm and the other of 685 nm. We used the first at $T_{\text{laser}} \approx 20$ °C ($\lambda = 690$ nm) and the second at $T_{\text{laser}} \approx -10$ °C ($\lambda = 682$ nm). The bandwidth of these diode lasers is ~ 3 MHz. For delay times longer than 200 ms, a cw single-frequency dye laser (Coherent 599–21 with an intracavity assembly, bandwidth $\Gamma_{\text{laser}} \approx 2$ MHz, dye DCM) pumped by an Ar^+ laser (Coherent, Innova 310) was used. The speed of the frequency scan of this dye laser is limited by piezoelectric-driven mirrors to ~ 100 MHz/ms, which is 10^4 – 10^5 times slower than that of diode lasers.

For delay times shorter than 30 s, the burn and probe pulses were obtained by means of two acoustooptic modulators (AOMs, Isomet 1206C, center frequency = 110 MHz) in series (suppression of laser intensity through the AOMs when switched

off was better than 10^6). For delay times longer than 30 s, no AOMs were used and the intensity of the probe pulse was reduced by using an optical density filter. The area of the laser beam on the sample was $A \approx 0.5 \text{ cm}^2$.

Burning-power densities in the range from $P/A \approx 50 \text{ nW/cm}^2$ to 5 mW/cm^2 were used, with burning times varying from $t_b = 10 \mu\text{s}$ to 30 s. Thus, burning-fluence densities varied between $Pt_b/A \approx 3 \text{ nJ/cm}^2$ and 10 mJ/cm^2 . The holes were detected in fluorescence excitation with a cooled photomultiplier (PM, EMI 9658R). To separate the fluorescence signal from the scattered laser light, a few long-wavelength pass filters were used (Schott RG 715, total thickness $\approx 1.2 \text{ cm}$) such that $\lambda_{\text{det}} \geq 715 \text{ nm}$. The fluorescence excitation signals from the sample before and after burning were stored in two different channels of a digital oscilloscope (LeCroy 9360, bandwidth 300 MHz). The signals were averaged in different ways, depending on delay time. For delay times shorter than 30 s, a sequence of probe–burn–probe cycles (see Figure 2) was applied with an appropriate repetition rate $\leq 10 \text{ Hz}$. After each cycle, the frequency of the laser was slightly shifted (by about twice the holewidth) to obtain a fresh baseline for each hole to be burnt. Transient holes, which live about 1 ms (see below), were averaged 10^3 to 10^4 times. For persistent holes with $1 \text{ ms} \leq t_d \leq 30 \text{ s}$, the signals were averaged 50–100 times with the digital oscilloscope. If longer averaging is used, the signal of the baseline region decreases due to the presence of previously burnt holes. For delay times longer than 30 s, the signals were averaged point by point about 1000 times. In this case, the pulse scheme of Figure 2 was only used once and not cycled through.

The transient holes observed for delay times shorter than $\sim 5 \text{ ms}$ result from temporary population storage in the triplet state. The lifetime of the triplet state can be obtained by measuring the area of a transient hole as a function of delay time t_d . In the RC, the hole decays in $1.6 \pm 0.1 \text{ ms}$; in the CP47 it decays in $0.6 \pm 0.05 \text{ ms}$. These values are in good agreement with the triplet lifetimes reported in the literature, obtained by other methods.^{36,37}

2.3. Determination of the “Effective” Homogeneous Line Width from the Hole Width. Γ'_{hom} is determined in the following way: first, the holes burnt during a time t_b and probed after a delay time t_d are measured as a function of burning-fluence density Pt_b/A and their profiles fitted with Lorentzian curves. The holewidths Γ_{hole} are then extrapolated to $Pt_b/A \rightarrow 0$ to eliminate the effect of power broadening. This yields a value $\Gamma_{\text{hole},0}(t_b, t_d)$. Since the laser bandwidth $\Gamma_{\text{laser}} \approx 2 \text{ MHz} \ll \Gamma_{\text{hole}} \approx$ a few 100 MHz to a few GHz, we neglect Γ_{laser} . For $t_d > t_b$ ^{16,38}

$$\Gamma_{\text{hole},0}(t_b, t_d) = \Gamma'_{\text{hom}}(t_b) + \Gamma'_{\text{hom}}(t_d) \quad (1)$$

To determine Γ'_{hom} , we first perform a hole-burning experiment at delay time $t_d = t_b$. In this case, $\Gamma_{\text{hole},0}(t_b, t_b) = 2\Gamma'_{\text{hom}}(t_b)$. Inserting $\Gamma'_{\text{hom}}(t_b)$ from this equation into eq 1 yields

$$\Gamma'_{\text{hom}}(t_d) = \Gamma_{\text{hole},0}(t_b, t_d) - \frac{1}{2}\Gamma_{\text{hole},0}(t_b, t_b) \quad (2)$$

For $t_d < 30 \text{ s}$, we often used $t_b \approx t_d$ so that eq 2 reduces to $\Gamma'_{\text{hom}}(t_d) = \frac{1}{2}\Gamma_{\text{hole},0}(t_b, t_b)$.²⁰ The general expression of eq 2 has to be used whenever $t_d > t_b$. Note that for $t_d \gg t_b$, $\Gamma'_{\text{hom}}(t_d) \approx \Gamma_{\text{hole},0}(t_b, t_d)$ and not equal to one-half the hole width.

3. Results and Discussion

3.1. Temperature Dependence of Γ'_{hom} . Figure 3a shows the temperature dependence of the “effective” homogeneous line

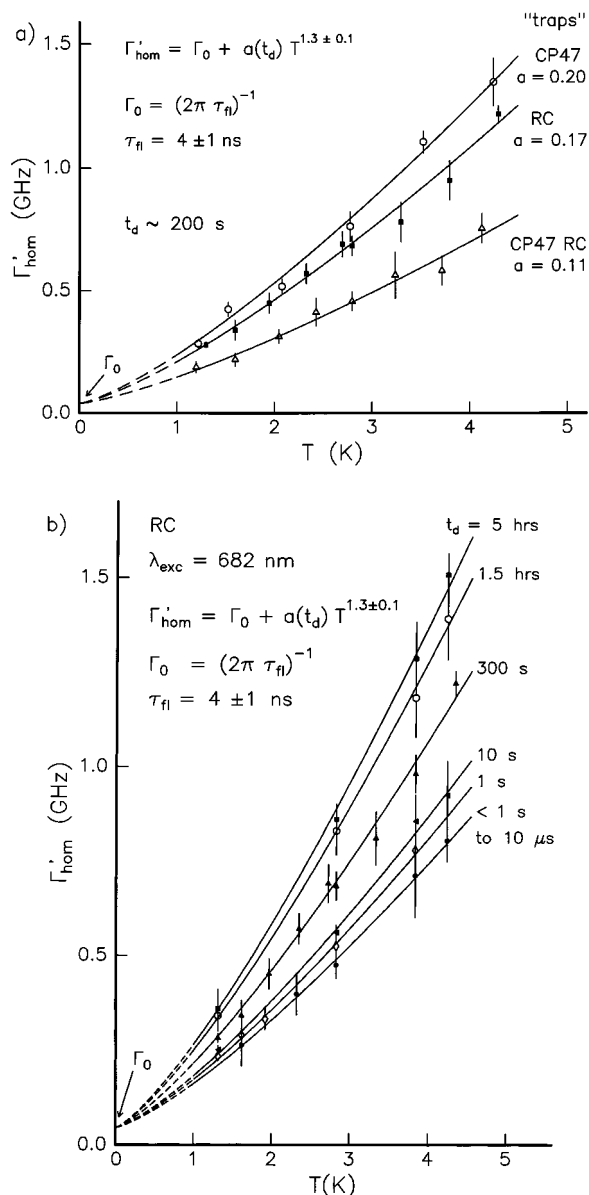


Figure 3. (a) Temperature dependence of Γ'_{hom} for the red-most absorbing trap pigments in the three complexes studied, at $t_d \approx 200 \text{ s}$. Γ'_{hom} follows a $T^{1.3 \pm 0.1}$ power law for all three complexes and extrapolates to $\Gamma_0 = (2\pi\tau_{\text{fl}})^{-1} = 40 \pm 10 \text{ MHz}$ for $T \rightarrow 0$, with $\tau_{\text{fl}} = 4 \pm 1 \text{ ns}$, the fluorescence lifetime of chlorophyll-like molecules. (b) Temperature dependence of Γ'_{hom} of the trap pigments of the RC at 682 nm for delay times t_d between 10 μs and 5 h. All curves follow a $T^{1.3}$ power law for a given delay time and extrapolate to $\Gamma_0 = (2\pi\tau_{\text{fl}})^{-1}$ for $T \rightarrow 0$, with τ_{fl} being the fluorescence lifetime of the pigment. The coupling constant $a(t_d)$ increases with delay time for $t_d \geq 1 \text{ s}$. For delay times $t_d < 1 \text{ s}$, all data points fall on the same curve, implying that there is no spectral diffusion in this time span (see also Figures 4a and 5).

width for the trap pigments of the three subcore complexes CP47, RC, and CP47 RC between 1.2 and 4.2 K for $t_d \approx 200 \text{ s}$. The complexes were excited at the maximum of their trap distributions, which is at 682 nm for the RC against 690 nm for CP47 and CP47 RC. The three curves extrapolate, within the error bars, to the same value $\Gamma_0 = (2\pi\tau_{\text{fl}})^{-1} = (40 \pm 10) \text{ MHz}$ for $T \rightarrow 0$, with $\tau_{\text{fl}} = 4 \pm 1 \text{ ns}$, the fluorescence lifetime of the “trap” pigments.^{20,29} They exhibit a $T^{1.3 \pm 0.1}$ power law dependence up to at least 4.2 K, which suggests that the pigment–protein interactions in these complexes are similar to those in organic amorphous systems at low temperature^{30,33,34,39} and determined by two-level-systems (TLSs).^{4,5,16,17} It is

interesting that picosecond vibrational echoes measured on myoglobin between 60 and 180 K obey the same power law.¹¹ One could think in first instance that this T dependence is determined by the surrounding glass (glycerol and buffer) in which the proteins are embedded. We have verified, as will be shown below, that this is not the case because the delay time dependence of Γ'_{hom} for the proteins is very different from that in glasses.

Although the T dependence of Γ'_{hom} is of the same form for all complexes, the coupling constant $a(t_d)$ (see eq 3) is different. For the isolated RC and CP47, this might be due to differences in the protein environment. Since the red-most trap pigment of the CP47 RC complex appears to be the same as that of CP47,²⁰ we would expect the value of $a(t_d)$ for CP47 RC to be equal to that of CP47, which is not true. Another possibility might be that the differences in $a(t_d)$ are due to a change in the coupling strength of the pigments to the protein in CP47 RC after chemical separation of CP47 and RC. It would be surprising, however, that this would lead to an increase of the coupling constant by almost a factor of 2. A third possibility is spectral diffusion, i.e., an increase of the value of Γ'_{hom} with delay time caused by structural relaxation of the protein. We will show below that this is the correct explanation.

Figure 3b shows Γ'_{hom} versus T data for the trap pigments of the RC for delay times between 10 μs and 5 h. Each curve follows a $T^{1.3\pm 0.1}$ dependence with a coupling constant $a(t_d)$ that increases with delay time. The results demonstrate that spectral diffusion does indeed occur in this complex but apparently not for delay times shorter than 1 s. This behavior is different from that in doped glasses, where we have observed SD to occur over 15 orders of magnitude in time, between 10^{-10} and 10^5 s.^{16,17,38} In the presence of spectral diffusion (SD), Γ'_{hom} can be expressed as^{16,38,39}

$$\Gamma'_{\text{hom}} = \Gamma_0 + a(t_d)T^{1.3\pm 0.1} = \Gamma_0 + [a_{\text{PD}} + a_{\text{SD}}(t_d)]T^{1.3\pm 0.1} \quad (3)$$

where a_{PD} is the "pure" dephasing contribution to Γ'_{hom} which accounts for fast fluctuations of the optical transition within the 4 ns lifetime of the pigment; a_{SD} is the delay time-dependent contribution to Γ'_{hom} responsible for spectral diffusion. The functional dependence of a_{SD} on delay time yields the distribution $P(R)$ of relaxation rates R in the protein. However, for delay times shorter than about 1 s, all data follow the same curve and, apparently, spectral diffusion does not occur in the RC complex at short times! This behavior is very different from that in doped glasses, where SD occurs over at least 15 orders of magnitude in time.^{16–18,38,40}

3.2. Delay-Time Dependence of Γ'_{hom} . Let us now look at the variation of Γ'_{hom} with delay time in more detail. Data for the RC are shown in Figure 4a on a logarithmic scale. For a given $T \leq 4.2$ K, Γ'_{hom} is constant from a few microseconds and ~ 1 s, like in crystalline systems. In the latter, Γ'_{hom} only increases with temperature but not with t_d .^{33,34} However, from $t_d \approx 1$ s up to 5 h, Γ'_{hom} appears to increase logarithmically with t_d , as found for glassy systems.^{16–18} Thus, for $t_d < t_{d,0} \approx 1$ s, the results seem to be determined by pure dephasing, i.e., by fast, local fluctuations. We infer from these results that the protein is rigid and behaves like a crystal in the direct surrounding of the excited pigments. The onset of SD at a delay time $t_{d,0} \approx 1$ s and the logarithmic delay-time dependence of Γ'_{hom} suggest that only slow fluctuations are involved in conformational relaxation at low temperatures, implying that protein motions in the RC have a broad and continuous distribution $1/R$ of low-frequency rates R with a cutoff at ~ 1

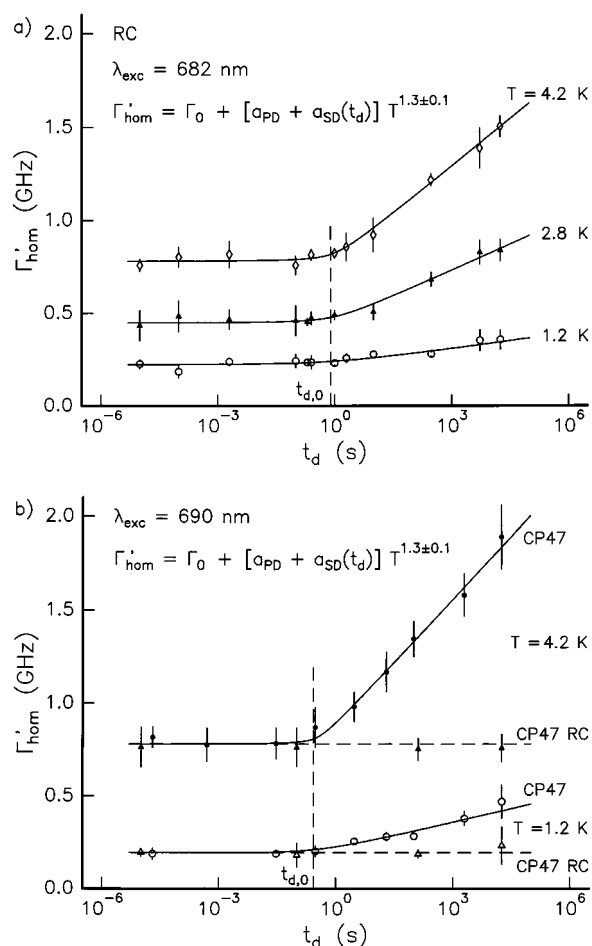


Figure 4. (a) Γ'_{hom} versus $\log t_d$ for the trap pigments of the RC at 1.2, 2.8, and 4.2 K. Γ'_{hom} is constant from $t_d \approx 10^{-5}$ s up to $t_d \approx 1$ s at a given temperature. This behavior is presumably determined by pure dephasing (PD) (see also Figure 5). For $t_d > 1$ s and up to at least 5 h, Γ'_{hom} appears to increase linearly with $\log t_d$. The slope or amount of spectral diffusion (SD) increases with temperature. (b) Γ'_{hom} vs $\log t_d$ for the red-most trap pigments of CP47 (circles and solid line) and CP47 RC at 690 nm (triangles and dashed line) at 1.2 and 4.2 K.

Hz. These motions probably take place at the interface between the protein and the buffer–glycerol glass, where there is more flexibility in the structure. As shown in Figure 4a, the delay time $t_{d,0}$ at which the onset of SD occurs does not depend on temperature below 4.2 K, which we interpret as an indication that protein modes with rates larger than 1 Hz are not thermally activated.

Figure 4b shows the delay-time dependence of Γ'_{hom} for the CP47 and CP47 RC complexes, at 1.2 and 4.2 K. Qualitatively, the results for CP47 are similar to those obtained for the isolated RC (see Figure 4a), but quantitatively they show differences. The onset of SD in CP47 starts at a somewhat shorter delay time ($t_{d,0} \approx 300$ ms) than in the RC ($t_{d,0} \approx 1$ s). We interpret this result as CP47 having protein motions with a slightly higher cutoff rate (~ 3 Hz) than the RC. Another difference is that for $t_d > t_{d,0}$ the slope $d\Gamma'_{\text{hom}}/d\log t_d$ at a given temperature is steeper for CP47 (protein mass ~ 70 kDa) than for the RC (~ 110 kDa), indicating that the amount of SD is larger for CP47. Surprisingly, CP47 RC (~ 180 kDa) shows *no* spectral diffusion over the whole time range investigated, from 10^{-5} to 10^5 s. It appears, therefore, to be rigid (only having fast, crystalline-like fluctuations) at $T \leq 4.2$ K. This is an interesting result because CP47 RC, which is larger than CP47, was excited at the same wavelength ($\lambda = 690$ nm) as CP47, which, contrary to CP47 RC, shows SD. The results suggest that spectral diffusion in

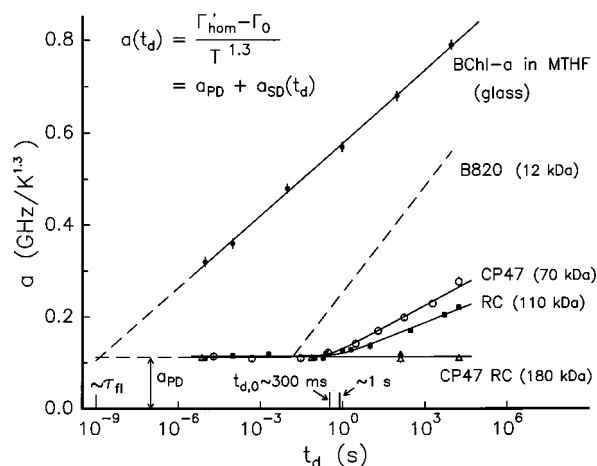


Figure 5. Coupling constant $a(t_d)$ as a function of $\log t_d$ for the trap pigments of the three PS II subcore complexes studied, the purple bacteria subunit B820,⁴² and the glass MTHF doped with BChl *a*.¹⁶ At $t_d \approx 200$ s, there are two data points (open and closed triangles) on the horizontal line. They correspond to holes burnt in different trap distributions of the CP47 RC complex: CP47 at 690 nm (open triangle) and RC at 682 nm (closed triangle). The value of $a(t_d)$ for the glassy system extrapolates to a_{PD} for $t_d \approx \tau_{fl} \approx 10^{-9}$ s.

these pigment–protein complexes involves the *whole* complex or a substantial part of it.

3.3. Comparison of Spectral Diffusion in the Three PS II Subcore Complexes with Doped Organic Glasses. In Figure 5 we have plotted the coupling constant $a(t_d) = a_{PD} + a_{SD}(t_d)$ as a function of $\log t_d$ for the three protein complexes together with results obtained for another protein (B820, see section 3.4) and for a doped organic glass (bacteriochlorophyll *a* (BChl *a*) in methyltetrahydrofuran (MTHF)¹⁶). The values were obtained from curves similar to those in Figure 3b, and with help of eq 3. It is striking that the slopes in Figure 5 appear to be correlated with the mass or size of the protein and not with the number of pigments in these proteins (8 in RC, ~ 14 in CP47, and ~ 22 in CP47 RC). For CP47 RC we have plotted two data points at $t_d = 200$ s for different wavelengths. The open triangle is the $a(t_d)$ value for the trap of the CP47 component within CP47 RC, which was obtained from the temperature dependence of Γ'_{hom} at 690 nm.²⁰ The closed triangle corresponds to the trap of the RC component in CP47 RC and was obtained from the temperature dependence of the holewidth at 682 nm.²⁰ Since the data point for excitation at 682 nm does not deviate significantly from the horizontal line drawn through the 690 nm data points of CP47 RC, we conclude that the SD behavior is characteristic for the entire complex or a large part of it and does not depend on the particular trap pigment actually excited.

For the doped organic glass, we have chosen BChl *a* in MTHF because BChl *a* is similar to Chl *a* and MTHF is a “normal” glass.¹⁶ The t_d dependence of the coupling constant $a(t_d)$ is quite different for the glass as compared to that for the protein complexes. For the glass, $\Gamma'_{hom} \propto \log t_d$ between at least 10^{-9} s and 10^5 s; also, there is significantly more SD in the glass than in the PS II subcore complexes. The observations made for MTHF are equally valid for other organic glasses.^{16,18,39} If we extrapolate the coupling constant $a(t_d)$ for BChl *a* in MTHF to short delay times, it reaches its a_{PD} value at $t_d \approx \tau_{fl} \approx 10^{-9}$ s.¹⁶ This value is equal to the $a(t_d)$ value to which the three protein curves merge at $t_d \leq t_{d,0} \approx 300$ ms to 1 s. We assume here that pure dephasing, which is determined by fast, local fluctuations, remains as the only dephasing mechanism in the proteins for $t_d < t_{d,0}$; i.e., there is no spectral diffusion in these complexes at short times.

If we assume that the amount of spectral diffusion (SD) is proportional to the pigment–protein interaction—probably of a multipolar type ($\propto 1/r^n$ with $n \geq 3$)—and to the number of two-level systems present at the surface ($\propto r^2$), we conclude that $SD \propto 1/r^{n-2}$, i.e., the slope da/dt should decrease with the size of the protein and, for a constant density, also with the mass, as experimentally observed.

3.4. Comparison with Other Photosynthetic Proteins and Myoglobin. The correlation which we have found between the amount of SD and the mass of the protein suggests that the entire protein or a large part of it is involved in the slow fluctuations. The rate and the amplitude of such motions presumably decrease with an increase of the mass of the protein.

Qualitatively, very similar SD results to those presented here have been found in our group for the B820 dimer and the B777 monomer subunits of the LH1 light-harvesting core complex of purple bacteria.^{41,42} The dashed curve in Figure 5 represents data for B820. For this complex the amount of SD is much larger and the onset of SD occurs at shorter delay times than in the PS II subcore complexes of green plants, probably because B820 is a much smaller protein (mass ~ 12 kDa).

The SD results on the photosynthetic protein complexes discussed here differ from those reported for substituted myoglobins obtained by other techniques. In particular, Zn mesoporphyrin IX substituted myoglobin investigated by three-pulse photon echoes between 10^{-10} and 10^{-1} s, at temperatures between 1.7 and 23 K, shows several steps in the dependence of Γ'_{hom} on $\log t_d$ that shift to shorter delay times with increasing temperature according to an Arrhenius law.^{8–10} These results were interpreted in terms of sharp and well-defined relaxation rates thought to play a role in these proteins. On the other hand, temperature-cycling hole-burning experiments on free-base protoporphyrin IX substituted myoglobin in the 100 mK region carried out on a much longer time scale (between minutes and 10 days) suggested a smooth increase of the holewidth with time.^{12,13} We are planning experiments to find out whether the differences are due to the nature of the proteins involved or to the different techniques and time scales used.

4. Conclusions

We have shown that protein dynamics at low temperature can be studied by high-resolution time-resolved hole-burning covering 10 orders of magnitude in time, from microseconds to many hours.

The “effective” homogeneous line width yields a $T^{1.3 \pm 0.1}$ power law in the range 1.2–4.2 K for any given delay time, as in doped organic glasses, indicating that TLSs are responsible for the dephasing. The dependence of Γ'_{hom} on t_d , however, is quite different. While glassy systems show a linear dependence of Γ'_{hom} on $\log(t_d)$ over at least 15 orders of magnitude (between $\sim 10^{-9}$ and 10^5 s), this is not true for photosynthetic protein complexes. For delay times $t_d \leq 300$ ms, Γ'_{hom} remains constant at a given temperature and the protein dynamics are reminiscent of that in crystalline systems: only pure dephasing takes place, i.e., only fast, local fluctuations during the excited-state lifetime occur. For $t_d \geq 300$ ms, spectral diffusion may set in depending on the protein. CP47 RC does not undergo SD within the time span investigated here, i.e., there are no conformational changes at $T \leq 4.2$ K in this protein and only fast, local fluctuations typical of a rigid system occur. The smaller RC and CP47 complexes do show spectral diffusion for delay times $t_d \geq 1$ s and ≥ 300 ms, respectively. Thus, slow motions involving the entire protein or a substantial part of it take place in these systems at low temperatures. The SD

behavior at delay times longer than $t_{d,0}$ appears to be similar to that in glasses: the distribution of low-frequency relaxation rates is very broad and continuous, $P(R) \propto 1/R$, and has a cutoff frequency of 1–3 Hz. This behavior is different from that reported for Zn-substituted myoglobin by three-pulse photon echoes.^{8,9}

The amount of SD, furthermore, appears to be correlated with the mass of the protein and probably involves TLSs active at the more flexible protein–buffer/glycerol interface. The inner part of these proteins is probably rigid at low temperatures.

Acknowledgment. The present experiments have been carried out with RC, CP47, and CP47 RC samples prepared by H. van Roon at the Department of Biophysics of the Free University Amsterdam in the context of our joint study on energy transfer and trapping in these complexes.²⁰ We thank her, R. van Grondelle, and J. P. Dekker for the kind supply of these materials. W. C. A. Vrouwenfelder is acknowledged for his help in some of the experiments. We further thank R. J. Silbey for enlightening discussions concerning the interpretation of the spectral diffusion results and J. H. van der Waals for critical comments on the manuscript and helpful suggestions. The investigations were supported by The Netherlands Foundation for Physical Research (FOM) and Chemical Research (SON) with financial aid from The Netherlands Organization for Scientific Research (NWO).

References and Notes

- Frauenfelder, H.; Sligar, S. G.; Wolynes, P. G. *Science* **1991**, *254*, 1598.
- Frauenfelder, H.; Wolynes, P. G. *Phys. Today* **1994**, *47*, 58.
- Elber, R.; Karplus, M. *Science* **1987**, *235*, 318.
- Anderson, P. W.; Halperin, B. I.; Varma, C. M. *Philos. Mag.* **1972**, *25*, 1.
- Phillips, W. A. *J. Low Temp. Phys.* **1972**, *7*, 351.
- Ansari, A.; Berendzen, J.; Bowne, S. F.; Frauenfelder, H.; Iben, I. E. T.; Sauke, T. B.; Shyamsunder, E.; Young, R. D. *Proc. Natl. Acad. Sci. U.S.A.* **1985**, *82*, 5000.
- Thorn Leeson, D.; Berg, O.; Wiersma, D. A. *J. Phys. Chem.* **1994**, *98*, 3913.
- Thorn Leeson, D.; Wiersma, D. A. *Phys. Rev. Lett.* **1995**, *74*, 2138.
- Thorn Leeson, D.; Wiersma, D. A. *Nat. Struct. Biol.* **1995**, *2*, 848.
- Thorn Leeson, D.; Wiersma, D. A.; Fritsch, K.; Friedrich, J. *J. Phys. Chem. B* **1997**, *101*, 6331.
- Rella, C. W.; Kwok, A.; Rector, K.; Hill, J. R.; Schweteman, H. A.; Dlott, D. D.; Fayer, M. D. *Phys. Rev. Lett.* **1996**, *77*, 1648.
- Gafert, J.; Pschierer, H.; Friedrich, J. *Phys. Rev. Lett.* **1995**, *74*, 3704.
- Fritsch, K.; Friedrich, J.; Parak, F.; Skinner, J. L. *Proc. Natl. Acad. Sci. U.S.A.* **1996**, *93*, 15141.
- Shibata, Y.; Kurita, A.; Kushida, T. *J. Chem. Phys.* **1996**, *104*, 4396.
- Shibata, Y.; Kurita, A.; Kushida, T. *Biophys. J.* **1998**, *75*, 521.
- Koedijk, J. M. A.; Wannemacher, R.; Silbey, R. J.; Völker, S. *J. Phys. Chem.* **1996**, *100*, 19945 and references therein.
- Silbey, R. J.; Koedijk, J. M. A.; Völker, S. *J. Chem. Phys.* **1996**, *105*, 901 and references therein.
- Littau, K. A.; Dugan, M. A.; Chen, S.; Fayer, M. D. *J. Chem. Phys.* **1992**, *96*, 3484 and references therein.
- Hankamer, B.; Barber, J.; Boekema, E. J. *Annu. Rev. Plant Physiol. Plant Mol. Biol.* **1997**, *48*, 641 and references therein.
- Den Hartog, F. T. H.; Dekker, J. P.; Van Grondelle, R.; Völker, S. *J. Phys. Chem.* **1998**, *102*, 11007.
- Kühlbrandt, W.; Wang, D. N.; Fujiyoshi, Y. *Nature* **1994**, *367*, 614.
- Rhee, K. H.; Morris, E. P.; Zheleva, D.; Hankamer, B.; Kühlbrandt, W.; Barber, J. *Nature* **1997**, *389*, 522.
- Boekema, E. J.; Van Roon, H.; Dekker, J. P. *FEBS Lett.* **1998**, *424*, 95.
- Eijkelhoff, C.; Dekker, J. P. *Biochim. Biophys. Acta* **1995**, *1231*, 21 and references therein.
- Bricker, T. M. *Photosynth. Res.* **1990**, *24*, 1.
- Kwa, S. L. S.; Van Kan, P. J. M.; Groot, M. L.; Van Grondelle, R.; Yocum, C. F.; Dekker, J. P. In *Research in Photosynthesis*; Murata, N., Ed.; Kluwer: Dordrecht, 1992; Vol 1, p 263.
- Chang, H.-C.; Jankowiak, R.; Yocum, C. F.; Picorel, R.; Alfonso, M.; Seibert, M.; Small, G. J. *J. Phys. Chem.* **1994**, *98*, 7717.
- Eijkelhoff, C.; Dekker, J. P.; Boekema, E. J. *Biochim. Biophys. Acta* **1997**, *1321*, 10.
- Groot, M. L.; Dekker, J. P.; Van Grondelle, R.; Den Hartog, F. T. H.; Völker, S. *J. Phys. Chem.* **1996**, *100*, 11488.
- Wannemacher, R.; Koedijk, J. M. A.; Völker, S. *Chem. Phys. Lett.* **1993**, *206*, 1 and references therein.
- Völker, S.; Macfarlane, R. M.; Genack, A. Z.; Trommsdorf, H. P.; van der Waals, J. H. *J. Chem. Phys.* **1977**, *67*, 1759.
- Völker, S.; Macfarlane, R. M.; van der Waals, J. H. *Chem. Phys. Lett.* **1978**, *58*, 8.
- Völker, S. In *Relaxation Processes in Molecular Excited States*; Fünfschilling, J., Ed.; Kluwer: Dordrecht, 1989; p 113 and references therein.
- Völker, S. *Annu. Rev. Phys. Chem.* **1989**, *40*, 499 and references therein.
- Dekker, J. P.; Betts, S. D.; Yocum, C. F.; Boekema, E. J. *Biochemistry* **1990**, *29*, 3220.
- Groot, M. L.; Peterman, E. J. G.; Van Stokkum, I. H. M.; Dekker, J. P.; Van Grondelle, R. *Biophys. J.* **1995**, *68*, 281 and references therein.
- Groot, M. L.; Peterman, E. J. G.; Van Kan, P. J. M.; Van Stokkum, I. H. M.; Dekker, J. P.; Van Grondelle, R. *Biophys. J.* **1994**, *67*, 318.
- Creemers, T. M. H.; Koedijk, J. M. A.; Chan, I. Y.; Silbey, R. J.; Völker, S. *J. Chem. Phys.* **1997**, *107*, 4797.
- Den Hartog, F. T. H.; Van Papendrecht, C.; Silbey, R. J.; Völker, S. *J. Chem. Phys.* **1999**, *110*, 1010.
- Meijers, H. C.; Wiersma, D. A. *J. Chem. Phys.* **1994**, *101*, 6927.
- Störkel, U.; Creemers, T. M. H.; Den Hartog, F. T. H.; Völker, S. *J. Lumin.* **1998**, *76/77*, 327.
- Creemers, T. M. H.; Störkel, U.; Musa, S.; Visschers, R. W.; Völker, S. To be published.